Article ID: 1007-4627(2017) 02-0148-06

Multiple Internal Reflections Method in Analysis of Nuclear Reactions

ZHANG Pengming[1], SUN Qing[1], Sergei P. Maydanyuk[1,2]

(*1. Institute of Modern Physics, Chinese Academy of Sciences, Lanzhou 730000, China;*
2. Institute for Nuclear Research, National Academy of Sciences of Ukraine, Kiev 03680, Ukraine)

Abstract: In this paper we give a short review of the Method of Multiple of Internal Reflections (MIR method), which is accepted as the more accurate and rich in quantum description of nuclear reactions today. For a capture of the α particles by nuclei our approach gives (1) new parameters of the α–nucleus potential and (2) new fusion probabilities. We demonstrate that a fully quantum description of this process provided by the MIR method, and inclusion of probabilities of fusion into formalism allow to essentially increase agreement between theory and experimental data. In particular, our method found new parametrization and fusion probabilities and decreased the error by 41.72 times for $\alpha+^{40}$Ca and 34.06 times for $\alpha+^{44}$Ca in a description of experimental data in comparison with existing results. Based on our proposed fusion probability formula, we explain the difference between experimental cross-sections for $\alpha+^{40}$Ca and $\alpha+^{44}$Ca, which is connected with the theory of coexistence of the spherical and deformed shapes in the ground state for nuclei near the neutron magic shell $N=20$. To obtain deeper insight into the physics of nuclei with the new discovered magic number $N=26$, we predict new cross-section of $\alpha+^{46}$Ca for further experimental confirmation.

Key words: alpha-capture; tunneling effect; multiple internal reflection; fusion probability; coefficient of penetrability and reflection; sharp angular momentum cut off; alpha-decay

CLC number: O571.6; **Document code:** A **DOI:** 10.11804/NuclPhysRev.34.02.148

1 Introduction

Our understanding about nuclear interactions is based on experimental information about nuclear reactions. Today, semiclassical methods are very popular in quantum description of these reactions (decays of nuclei with emission of protons, α particles or more heavy fragments, elastic and inelastic scattering, fission, synthesis of superheavy nuclei, capture of α particles or other fragments by nuclei, *etc.*) and analysis [1]. However, practically, methods more accurate than the semiclassical approach of the first order [*i.e.* Wentzel - Kramers - Brillouin (WKB) approximation] are never used in calculations. For example, theoretical estimations of half-lives of the α decay of more than 340 nuclei (and more than 1240 predicted half-lives, see Ref. [2]) based on such semiclassical approaches form a basis of existed nuclear databases[3, 4].

However, a region of applicability of WKB-approximation (in determination of wave functions) does not include internal region of nucleus which is involved to the studied reaction. As a result, internal structure of nucleus is hidden for quantum analysis, if to use such approximations. By such a reason, the semiclassical wave functions, obtained after extrapolation into nuclear region with small distances, are essentially different from the wave functions obtained using methods of quantum mechanics. Also, in estimation of half-lives of the α decay (and cross-sections of inverse processes), the WKB-approximation neglects a role of initial (final) conditions in determination of the wave function describing nuclear process (that excludes a possibility to study dynamics). Perturbative approaches inside such space nuclear regions cannot be applied also. All such reasons cause interest in developments of the accurate method of quantum mechanics beyond the semiclassical approximations above. It turns out that role of quantum corrections to the semiclassical wave functions (obtained via methods of quantum mechanics) in nuclear tasks is more essential than

Received date: 16 Nov. 2016; **Revised date:** 5 Dec. 2016
Foundation item: National Natural Science Foundation of China(11575254)
Biography: ZHANG Pengming(1976–), male, Xuzhou, Jiangsu, Professor, working on high energy and nuclear physics; E-mail: zhpm@impcas.ac.cn.

inclusion of nuclear deformations, different terms in construction of nuclear potentials.

In this paper we review a Method of Multiple Internal Reflections (MIR method, see Refs. [5–8]), analyze its peculiarities in a task of capture of the α particles by nuclei. We show that (1) the fully quantum description of the α-capture process, and (2) inclusion of probabilities of fusion allows to essentially increase agreement between theory and experiment.

2 Method of multiple internal reflections

We shall analyze the Method of multiple internal reflections in the task of capture of the α-particle by the nucleus in a spherically symmetric scenario*. To apply the idea of multiple internal reflections to study packet tunneling through complicated realistic barriers, let us consider the radial barrier of an arbitrary shape, which has successfully been approximated by a sufficiently large number N of rectangular steps:

$$V(r) = \begin{cases} V_1 & \text{at } r_{\min} < r \leqslant r_1 \quad \text{(region 1)}, \\ \dots & \dots \qquad\qquad\qquad \dots \\ V_{\rm N} & \text{at } r_{N-1} \leqslant r \leqslant r_{\max} \quad \text{(region } N\text{)}, \end{cases} \tag{1}$$

where V_j are constants ($j = 1 \dots N$)†. Let us denote the first region with a left boundary at point $r_{\min}$ (we denote it also as $r_{\rm capture}$), and we shall assume that the capture of the α-particle by the nucleus in this region occurs after its tunneling through the barrier. We shall be interested in solutions for the above barrier energies, while the solution for tunneling could be subsequently obtained by changing $i\xi_i \to k_i$. A general solution of the wave function (up to its normalization) has the following form:

$$\psi(r,\theta,\varphi) = \frac{\chi(r)}{r} Y_{lm}(\theta,\varphi),\ \chi(r) = \begin{cases} \alpha_1 \mathrm{e}^{\mathrm{i}k_1 r} + \beta_1 \mathrm{e}^{-\mathrm{i}k_1 r}, & \text{at } r_{\min} < r \leqslant r_1 \quad \text{(region 1)}, \\ \dots & \dots \qquad\qquad \dots \\ \alpha_{N-1} \mathrm{e}^{\mathrm{i}k_{N-1} r} + \beta_{N-1} \mathrm{e}^{-\mathrm{i}k_{N-1} r}, & \text{at } r_{\rm N-2} \leqslant r \leqslant r_{N-1} \quad \text{(region } N-1\text{)}, \\ \mathrm{e}^{-\mathrm{i}k_{\rm N} r} + A_{\rm R} \mathrm{e}^{\mathrm{i}k_{\rm N} r}, & \text{at} r_{N-1} \leqslant r \leqslant r_{\max} \quad \text{(region } N\text{)}, \end{cases} \tag{2}$$

where α_j and β_j are unknown amplitudes, $A_{\rm T}$ and $A_{\rm R}$ are unknown amplitudes of transition and reflection, $Y_{lm}(\theta,\varphi)$ is the spherical function, and $k_j = \frac{1}{\hbar}\sqrt{2m(\tilde{E} - V_j)}$ are complex wave numbers. We have fixed the normalization so that the modulus of amplitude of the starting wave $\mathrm{e}^{-\mathrm{i}k_N r}$ equals unity. We shall search a solution to this problem by the multiple internal reflections approach.

According to the multiple internal reflections method, the scattering of a particle on the barrier is sequentially considered by steps of propagation of the wave packet relative to each boundary of the barrier (the idea of this approach can be understood most clearly in the problem of tunneling through the simplest rectangular barrier, see Refs. [6, 7], where one can find proof of this fully quantum exactly solvable method and analyze its properties). Each step in such a consideration of packet propagation is similar to one of the first independent $2N-1$ steps. From the analysis of these steps, we find recurrent relations for the calculation of the unknown amplitudes $A_T^{(n)}$, $A_R^{(n)}$, $\alpha_j^{(n)}$ and $\beta_j^{(n)}$ for an arbitrary step with number n (here, index j corresponds to the number of region V_j, and the logic of the definition of these amplitudes can be found in Ref. [8]). In the summation of these relations from each step, we impose the continuity condition for the full (summarized) wave function and its derivative relative to the corresponding boundary.

According to the analysis of waves propagating in a region with an arbitrary number j on the arbitrary step, each wave can be represented as a multiplication of the exponential factor $\mathrm{e}^{\pm \mathrm{i}k_j r}$ and constant amplitude. In practical calculations, the difficulty consists in the determination of these unknown amplitudes. However, to make such calculations as easy as possible for an arbitrary step, one can rewrite the amplitude of the wave that has transmitted through the boundary with number j as the product of the amplitude of the corresponding wave incident on this boundary and the new factor $T_j^{\pm}$ (*i. e.*, the amplitude of transition through the boundary with number j). The bottom index indicates the number of the boundary, and the upper sign "+" or "−" is the direction of the incident wave to the right or left, respectively. We associate the amplitude of the reflected wave from the boundary with

*The role of nuclear deformations in the determination of the fusion probabilities in the α-capture task is analyzed in Ref. [5]

†We used this approximation for barriers of the proton and α-decay for the number of nuclei, where the width of each step is equal to 0.01 fm, and we demonstrated the stability of the calculations of all amplitudes of the wave function and penetrability[8]. We thus have effective tools for a detailed study of the quantum processes of tunneling and penetrability.

number j with the amplitude of the wave incident on this boundary via new factors $R_j^{\pm}$. The coefficients $T_1^{\pm}$, $T_2^{\pm}$, $T_3^{\pm}\dots$ and $R_1^{\pm}$, $R_2^{\pm}$, $R_3^{\pm}\dots$ can be found from the recurrence relations shown above[8]. We calculate $T_1^{\pm}$, $T_2^{\pm}$ $\dots T_{N-1}^{\pm}$ and $R_1^{\pm}$, $R_2^{\pm}$ $\dots R_{N-1}^{\pm}$ as

$$\begin{aligned}
T_j^{+} &= \frac{2k_j}{k_j+k_{j+1}}\,\mathrm{e}^{\mathrm{i}(k_j-k_{j+1})r_j} ,\\
T_j^{-} &= \frac{2k_{j+1}}{k_j+k_{j+1}}\,\mathrm{e}^{\mathrm{i}(k_j-k_{j+1})r_j} ,\\
R_j^{+} &= \frac{k_j-k_{j+1}}{k_j+k_{j+1}}\,\mathrm{e}^{2\mathrm{i}k_j r_j} ,\\
R_j^{-} &= \frac{k_{j+1}-k_j}{k_j+k_{j+1}}\,\mathrm{e}^{-2\mathrm{i}k_{j+1} r_j} .
\end{aligned} \tag{3}$$

Now, we consider the wave propagating in region with number j, which is incident from the right on the potential barrier with the right boundary at point r_{j-1} (and left boundary at point r_1). Let us find the wave reflected from this complicated barrier. This wave should combine all waves formed as a result of multiple internal reflections and propagations relative boundaries $r_1 \dots r_{j-1}$ and leave such a barrier. We define the reflection amplitude $\tilde{R}_{j-1}^{+}$ of such a summarized wave as

$$\begin{aligned}
\tilde{R}_{j-1}^{+} &= R_{j-1}^{+} + T_{j-1}^{+}\tilde{R}_j^{+}T_{j-1}^{-}\Big(1+\sum_{m=1}^{+\infty}(\tilde{R}_j^{+}R_{j-1}^{-})^m\Big)\\
&= R_{j-1}^{+} + \frac{T_{j-1}^{+}\tilde{R}_j^{+}T_{j-1}^{-}}{1-\tilde{R}_j^{+}R_{j-1}^{-}}.
\end{aligned} \tag{4}$$

Correspondingly, we calculate

$$\begin{aligned}
\tilde{R}_{j+1}^{-} &= R_{j+1}^{-} + T_{j+1}^{-}\tilde{R}_j^{-}T_{j+1}^{+}\Big(1+\sum_{m=1}^{+\infty}(R_{j+1}^{+}\tilde{R}_j^{-})^m\Big)\\
&= R_{j+1}^{-} + \frac{T_{j+1}^{-}\tilde{R}_j^{-}T_{j+1}^{+}}{1-R_{j+1}^{+}\tilde{R}_j^{-}} ,\\
\tilde{T}_{j+1}^{+} &= \tilde{T}_j^{+}T_{j+1}^{+}\Big(1+\sum_{m=1}^{+\infty}(R_{j+1}^{+}\tilde{R}_j^{-})^m\Big)\\
&= \frac{\tilde{T}_j^{+}T_{j+1}^{+}}{1-R_{j+1}^{+}\tilde{R}_j^{-}},\\
\tilde{T}_{j-1}^{-} &= \tilde{T}_j^{-}T_{j-1}^{-}\Big(1+\sum_{m=1}^{+\infty}(R_{j-1}^{-}\tilde{R}_j^{+})^m\Big)\\
&= \frac{\tilde{T}_j^{-}T_{j-1}^{-}}{1-R_{j-1}^{-}\tilde{R}_j^{+}} .
\end{aligned} \tag{5}$$

In such a summation, we have recurrent relations, which connect all amplitudes. We now choose the following values

$$\begin{aligned}
\tilde{R}_{N-1}^{+} &= R_{N-1}^{+} ,\ \tilde{R}_1^{-} = R_1^{-} ,\\
\tilde{T}_1^{+} &= T_1^{+} ,\ \tilde{T}_{N-1}^{-} = T_{N-1}^{-} ,
\end{aligned} \tag{6}$$

as our starting point and consequently calculate all amplitudes $\tilde{R}_{\mathrm{N}-2}^{+} \dots \tilde{R}_1^{+}$, $\tilde{R}_2^{-}$ $\dots \tilde{R}_{N-1}^{-}$ and $\tilde{T}_2^{+}$ $\dots \tilde{T}_{N-1}^{+}$. We find the coefficients α_j and β_j:

$$\begin{aligned}
\alpha_j &= \sum_{n=1}^{+\infty}\alpha_j^{(n)} = \tilde{T}_{j-1}^{+}\Big(1+\sum_{m=1}^{+\infty}(R_j^{+}\tilde{R}_{j-1}^{-})^m\Big)\\
&= \frac{\tilde{T}_{j-1}^{+}}{1-R_j^{+}\tilde{R}_{j-1}^{-}} = \frac{\tilde{T}_j^{+}}{T_j^{+}},\\
\beta_j &= \alpha_j \cdot R_j^{+} ,
\end{aligned} \tag{7}$$

the amplitudes A_{T} and A_{R} of transition and reflection concerning the barrier, and the corresponding coefficients of penetrability T_{MIR}‡ and reflection R_{MIR}:

$$A_{\mathrm{T}} = \sum_{n=1}^{+\infty}A_{\mathrm{T}}^{(n)} = \tilde{T}_1^{+} ,\quad A_{\mathrm{R}} = \sum_{n=1}^{+\infty}A_{\mathrm{R}}^{(n)} = \tilde{R}_{N-1}^{+} ,$$

$$T_{\mathrm{MIR}} \equiv \frac{k_N}{k_1}\left|A_{\mathrm{T}}\right|^2, \quad R_{\mathrm{MIR}} \equiv \left|A_{\mathrm{R}}\right|^2 . \tag{8}$$

We check the property

$$T_{\mathrm{MIR}} + R_{\mathrm{MIR}} = 1 , \tag{9}$$

which indicates whether the MIR method gives the proper solutions for the wave function (we obtain coincident amplitudes of the wave function calculated by MIR approach, with corresponding amplitudes obtained in the standard approach of quantum mechanics up to the first 15 digits). This is an important test confirming the reliability of the MIR method. So, we have obtained the full coincidence between the solutions for all amplitudes obtained by the MIR approach and the standard approach of quantum mechanics.

The cross-section of capture that includes the fusion of the α-particles with nuclei can be defined as[9]

$$\sigma_{\mathrm{capture}}(E) = \frac{\pi\hbar^2}{2m\tilde{E}}\sum_{l=0}^{l_{\max}}(2l+1)T_l P_l , \tag{10}$$

where E is the kinetic energy of the α-particle incident on the nucleus in the laboratory frame, $\tilde{E}$ is the kinetic energy of the relative motion of the α-particle of the nucleus in the center-of-mass frame (we use $E \simeq \tilde{E}$), m is the reduced mass of the α-particle and nucleus, P_l is the probability for fusion of the α-particle and nucleus, and T_l is the penetrability of the barrier. In the WKB approach, this coefficient is defined as

$$T_{\mathrm{WKB}}(\tilde{E}) = \exp\left\{-2\int_{R_2}^{R_3}\sqrt{\frac{2m}{\hbar^2}\left(\tilde{E}-V(r)\right)}\,\mathrm{d}r\right\} , \tag{11}$$

‡We shall analyze the penetrabilities and cross-sections obtained by the multiple internal reflections method and WKB method. To distinguish the calculated results, we shall add abbreviation “MIR” to the “multiple internal reflections method” and WKB to the WKB approach.

where R_2 and R_3 are the turning points determining the tunneling region.

3 Results

The cross-sections for $\alpha+{}^{44}$Ca calculated by the MIR and WKB approaches and experimental data[9] are presented in Fig. 1(a).

The MIR calculations with the included fusion probabilities found by the minimization method are added to this figure. One can see that the WKB approach gives higher values for the cross-section in comparison with the calculations from the MIR approach at $l_{\max}=10\sim15$. We conclude that the WKB approach gives reduced estimations for the fusion probabilities in comparison with the MIR approach. In Ref. [9] the effect of anomalous large-angle scattering (ALAS) was discussed, which was explained by the sharp angular momentum cut-off approach at some critical value of $l_{\max}$ (see Eqs. (1)$\sim$(2) in that paper). This case corresponds to calculations by the MIR approach at different values of $L_{\max}$ (where all fusion probabilities are equal to unity at $l\leqslant l_{\max}$). Here, curve 5 for $l_{\max}=10$ in Fig. 1(a) (and curve 6 for $l_{\max}=12$) is clearly better at describing the experimental data than curve 7 for $l_{\max}=15$ (which nearly coincides with subsequent calculations for higher $l_{\max}$). However, all these curves are far from the experimental data in comparison with curve 10, which includes the fusion probabilities obtained by the minimization method. Thus, the sharp angular momentum cutoff approach provides very restricted description of the experimental data for $\alpha+{}^{44}$Ca, while curve 10 is more successful. This result indicates that the dependence of the fusion probabilities on the angular momentum is more complicated and requires more careful study. The fusion probabilities obtained in our calculation of curve 10 are presented in Fig. 1(b). Our fusion probabilities are extracted by analyzing the experimental data inside the whole energy region, while Eberhard *et al.*[9] used only one fixed energy at $E=25$ MeV for analysis (and fusion probabilities are fixed to unity).

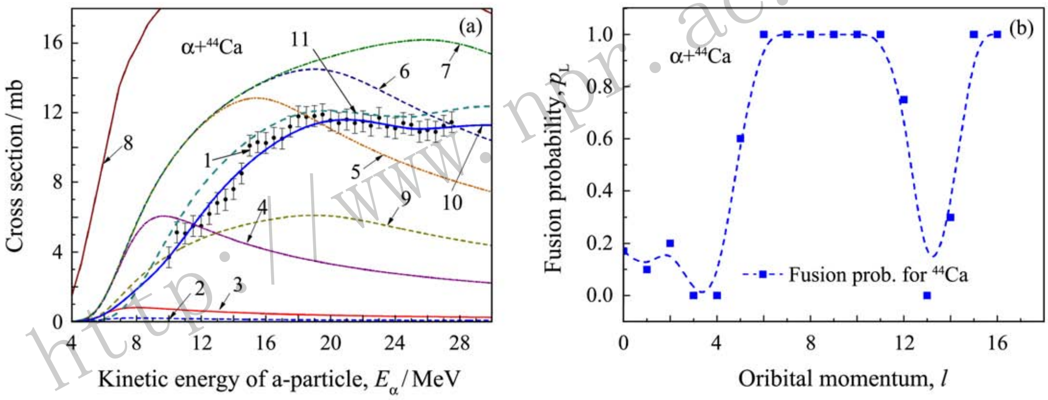

Fig. 1 (color online) Panel a: The capture cross-sections of the α-particle by the ^{44}Ca nucleus obtained by the MIR method and WKB approach (parameters of calculations: 10 000 intervals at $r_{\max}=70$ fm, parametrization from Ref. [10]). Here, the data labeled 1 are the experimental data extracted from [9], dashed blue line 2 is the cross-section at $l_{\max}=0$ short dotted red line 3 is the cross-section at $l_{\max}=1$, short dash-dotted purple line 4 is the cross-section at $l_{\max}=5$, dash double-dotted orange line 5 is the cross-section at $l_{\max}=10$, dashed dark blue line 6 is the cross-section at $l_{\max}=12$, dash dotted green line 7 is the cross-section at $l_{\max}=15$, solid brown line 8 is the cross-section at $l_{\max}=20$, dashed dark yellow line 9 is the normalized cross-section at $l_{\max}=17$, solid blue line 10 is the cross-section at $l_{\max}=17$, and dashed dark cyan line 11 is the cross-section at $l_{\max}=17$. The penetrabilities are calculated by the MIR method for lines $2\sim7$ and $9\sim11$, and by the WKB approach for line 8. Lines $10\sim11$ are obtained with the included fusion probabilities, and lines $2\sim9$ are obtained without the fusion probabilities. One can see that line 10, obtained after inclusion of the fusion probabilities, describes the experimental data with good accuracy. For line 11, the fusion probabilities are obtained by our formulas (21)–(27) in Ref. [5]). Panel b: The fusion probability for the capture of the α-particle by the ^{44}Ca nucleus obtained by the MIR approach (parameters of calculations: 10000 intervals at $r_{\max}=70$ fm, parametrization from Ref. [10]).

An important question addressed to applicability of the MIR approach is how much convergent solutions this method gives. In order to analyze this question, we calculate the penetrability $T_{\rm MIR}$ of the potential region (with the fixed internal boundary $r_{\min}$ and the external boundary $r_{\max}$) with the barrier in dependence of number of intervals N. Results of such calculations for the capture reaction $\alpha+{}^{44}$Ca at $l=0$ at a fixed energy of the α particle are given in Fig. 2. For analysis, we use a difference between two closest values of the penetrability, $Y(N)=T_{\rm MIR}(N-1)-T_{\rm MIR}(N)$, obtained at close numbers of intervals (used in vertical axis in that figure). One can see that at increasing number of intervals this difference decreases from 0.5 up to 10^{-10}! This means that at 100 000 intervals we obtain stable value for the penetrability where only 10 digit can be varied (and first 9 digits are stable). For each data, the reflection coefficient $R_{\rm MIR}$ is calculated independently, and a test is fulfilled (with accuracy of about $\big||T_{\rm MIR}+R_{\rm MIR}|-1\big|<10^{-15}$). This information characterizes accuracy of the MIR method. Of course, a famous Numerov' approach (popular in numeric calculations) cannot allow to reach such an accuracy.

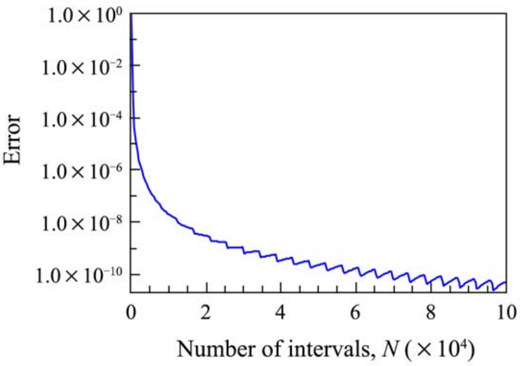

Fig. 2 (color online) The error $Y = |T_{\rm MIR}(N) - T_{\rm MIR}(N-1)|$ in calculations of the penetrability $T_{\rm MIR}(N)$ by the MIR method for the potential with the barrier with the internal boundary $r_{\rm min}$ and the external boundary $r_{\rm max}$ in dependence on number of intervals N for the capture of $\alpha+^{44}$Ca at the incident energy of the α particle of 5 MeV at $l=0$ (parameters of calculations: maximal number of radial intervals is $N=100\,000$, we obtained 500 data-points for curve; we fix boundaries as $r_{\rm min}=0.1$ fm and $r_{\rm max}=70$ fm for all calculations in this figure; a maximum of the barrier is 6.16 MeV, so we have tunneling at the studied energy of the α particle). Test $\big||T_{\rm MIR}+R_{\rm MIR}|-1\big|<10^{-15}$ is fulfilled for all data-points (where $R_{\rm MIR}$ is calculated independently by the MIR approach).

In order to describe the fusion in the studied α-capture reaction, we introduced a new formula for probability of complete fusion (for nuclei at close proton shells, see Ref. [5])

$$\begin{aligned} p_{\rm fus}(L) &= 1-p_1(L)-p_2(L)\ , \\ p_1(L) &= \frac{c_1}{1+{\rm e}^{(L-c_2)/c_3}}\ , \\ p_2(L) &= f_2(L)\cdot\sum_{n=1}{\rm e}^{-\dfrac{(L-n\cdot\varDelta)^2}{c_{4n}}}\ , \end{aligned} \qquad (12)$$

where $f_2(L)=1-{\rm e}^{-c_5\cdot(L-c_6)}$, $\varDelta = a\cdot(N-N_{\rm magic})+b$, and $a=2.31$, $b=4.05$, $c_1=1$, $c_2=4.2$, $c_3=0.5$, $c_{4n}=1$, $c_5=0.25$, $c_6=2.5$. Here, N is number of neutrons of the studied nucleus, and $N_{\rm magic}$ is the closest magic neutron number, where $N_{\rm magic}\leqslant N$ (*i. e.* $N_{\rm magic}=20$ for ^{40}Ca and ^{44}Ca). As we shown in Ref. [5], this formula provides different description of the fusion in the reactions for the α-capture by the ^{40}Ca and ^{44}Ca nuclei (we suppose this difference should be connected with the structure of the nucleus, which can be explained on the basis of the closure of nuclear shells). This aspect allows us to explain difference between the experimental cross-sections for capture by the ^{40}Ca and ^{44}Ca nuclei. We represent this result, our calculations and the corresponding existed experimental data in Fig. 3.

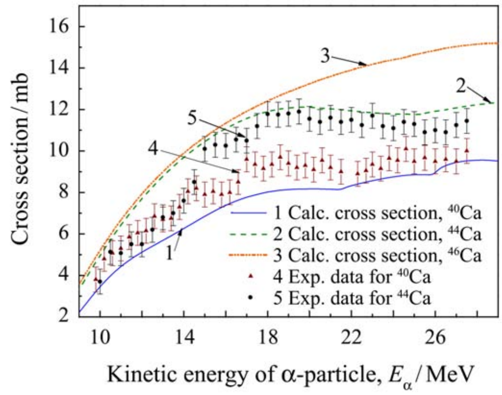

Fig. 3 (color online) The cross-sections calculated by the predicted formulas for the fusion probabilities for capture of the α-particle by the ^{40}Ca (see blue solid line 1), ^{44}Ca (see green dashed line 2) and ^{46}Ca (see orange dash-dotted line 3) nuclei obtained by the MIR method (parameters of calculations: 10 000 intervals at $r_{\rm max}=70$ fm). Here, the data labeled 4 and 5 are the experimental data for ^{40}Ca and ^{44}Ca extracted from Ref. [9].

In order to reinforce future investigations of fusion in such a type of reactions, on the basis of our formula (12) we provide also our prediction for the calculated cross-section for the α-capture by the ^{46}Ca nucleus (see orange line 3 in Fig. 3), which has never been measured. We choose the ^{46}Ca nucleus for such future measurements on the basis of the following motivation. Last years there are intensive research in understanding of the coexistence of the two shapes for the nuclei near the shells at $N=20$ and $N=28$, which lead to a reconsideration of main positions of the nuclear shell model and to the discovery of new magic numbers[11]. A review of this topic[11] gives interesting indications about the new neutron magic numbers at $N=16$ and $N=26$ and the properties of such nuclei (while the standard theory gives us only seven experimentally known neutron numbers at 2, 8, 20, 28, 50, 82, 126). So, it could be interesting to propose to investigate experimentally the fusion process at the capture of the α-particle by the ^{46}Ca nucleus. Such information could provide new insight into our understanding of physics of nuclei with such a neutron magic shell (and fusion for these nuclei).

4 Conclusions

In this paper we reviewed the Method of Multiple of Internal Reflections in quantum analysis of nuclear reactions. On example of capture of the α particle by the ^{44}Ca nucleus, we demonstrated that a fully quantum description of this process provided by the MIR method, and inclusion of probabilities of fusion into formalism allow to essentially increase agreement between theory and experimental data [this method found own parametrization, fusion probabilities and decreased error by 34.06 times in description of experimental data in comparison with other approaches (here we consider the maximally accurate WKB-calculations without the included probabilities of fusion, see line 8 in Fig. 1)]. In finishing, we add Fig. 2 where we show convergence of our calculations of the penetrability at increasing of number N of intervals for $\alpha+^{44}$Ca at the incident energy of the α particle of 5 MeV at $l=0$. In particular, one can see in this figure that the firth 9 digits in the calculated penetrability become stable at maximal chosen number of intervals of 100 000 (while at $N=50$ the second digit of the penetrability is changed). We provide our formula (12) of the fusion probabilities for the α-capture. On its basis we explain the differences between the cross-sections for $\alpha+^{40}$Ca and $\alpha+^{44}$Ca (see our calculated spectra given in Fig. 3 by blue solid line 1 and green dashed line 2 and experimental data 4 and 5 for these nuclei). To obtain deeper insight into the physics of nuclei with the new magic number $N=26$, we predict new cross-section of $\alpha+^{46}$Ca for further experimental confirmation (see orange dash-dotted line 3 in Fig. 3).

References:

[1] BALANTEKIN A B, TAKIGAWA N. Rev Mod Phys, 1998, **70**: 77.

[2] DENISOV V YU, KHUDENKO A A. Data Tables, 2009, **95**(6): 815.

[3] Available from: http://www.nndc.bnl.gov, http://www-nds.iaea.org/RIPL-2 .

[4] AUDI G, BERSILLON O, BLACHOT J, *et al.* Nucl Phys A, 2003, **729**(1): 3.

[5] MAYDANYUK S P, ZHANG P M, BELCHIKOV S V. Nucl Phys A, 2015, **940**: 89; arXiv: 1504.00567.

[6] OLKHOVSKY V S, MAYDANYUK S P. Ukr Phys Journ, 2000, **45**(10): 1262, nucl-th/0406035; MAYDANYUK S P, OLKHOVSKY V S, ZAICHENKO A K. Journ Phys Stud, 2002, **6**(1): 1; nucl-th/0407108.

[7] CARDONE F, MAIDANYUK S P, MIGNANI R, *et al.* Found Phys Lett, 2006, **19**(5): 441.

[8] MAYDANYUK S P, BELCHIKOV S V. Journ Mod Phys, 2011, **2**(6): 572, Journ Phys Stud, 2011, **15**(4), 40.

[9] EBERHARD K A, APPEL C, BANGERT R, *et al.* Phys Rev Lett, 1979, **43**(2): 107.

[10] DENISOV V YU, IKEZOE H. Phys Rev C, 2005, **72**(5): 064613, arXiv: nucl-th/0510082.

[11] PENIONZHKEVICH YU E, LUKYANOV S M. Phys Part Nucl, 2006, **37**: 240.

核反应中的多重内部反射方法研究

张鹏鸣[1,1)]，孙 清[1]，Sergei P. Maydanyuk[1,2]

(1. 中国科学院近代物理研究所，兰州 730000;
2. Institute for Nuclear Research, National Academy of Sciences of Ukraine, Kiev 03680, Ukraine)

摘要: 讨论了量子多重内部反射方法(MIR 方法)，这是一种研究核反应的更准确的量子力学方法。对于一个原子核俘获α粒子的过程，MIR 方法能够给出(1) α-核势的新参数；(2) 新的熔合几率。基于 MIR 方法我们给出了这类过程的完整量子力学描述，考虑熔合几率后 MIR 方法能够显著地提高实验与理论的吻合度。具体研究了$\alpha+^{40}$Ca 和$\alpha+^{44}$Ca 两类反应，给出了新的核势参数核和熔合几率。对于第一个反应理论计算值与实验的偏离比其他计算结果减少了 41.72 倍，对于第二个反应减少了 34.06 倍。进一步，基于本工作熔合几率公式，给出了两类反应截面不同的原因，这是与中子幻数 $N=20$ 附近的原子核基态的球形构型和形变构型共存导致的。为了更好地理解幻数 $N=26$ 附近原子核的性质，预言了$\alpha+^{46}$Ca 的反应截面。

关键词: α 粒子俘获；隧穿效应；多重内部反射方法；熔合几率；透射系数与反射系数；角动量截断；α 衰变

收稿日期: 2016-11-16; **修改日期:** 2016-12-05

基金项目: 国家自然科学基金资助项目(11575254)

1) E-mail: zhpm@impcas.ac.cn。